PERGAMON

International Journal of Multiphase Flow 27 (2001) 39–60

International Journal of Multiphase Flow

www.elsevier.com/locate/ijmulflow

Effect of surfactants on the instability of a liquid thread Part II: Extensional flow

S. Kwak, M.M. Fyrillas, C. Pozrikidis*

Department of Mechanical and Aerospace Engineering, University of California, San Diego, La Jolla, CA 92093-0411, USA

Received 7 October 1999; received in revised form 20 January 2000

Abstract

The effect of surfactants on the capillary instability of a liquid thread extending under the influence of an ambient flow is studied by linear theory for small-amplitude perturbations, numerical simulations for arbitrary amplitude perturbations based on boundary-integral and finite-volume methods, and numerical simulations based on an approximate model that relies on the long-wave approximation. Theoretical predictions and numerical simulations confirm previous predictions that, in the absence of surfactants, perturbations with a sufficiently small amplitude eventually decay as long as neither the viscosity of the thread nor the viscosity of the ambient fluid is equal to zero. It is shown, however, that for zero or infinite viscosity ratio, disturbances of any wavelength eventually amplify leading to thread breakup at a finite time. Surfactants stabilize the interface during the initial stages of the instability, but the increase in the mean surface tension due to surfactant dilution by stretching leads to higher perturbation amplitudes at long times. An asymptotic flow model is developed to describe the evolution of a viscous thread suspended in an ambient inviscid fluid subject to axisymmetric disturbances with long wavelength. Numerical solutions suggest that the similarity solution developed previously for a thread suspended in a quiescent fluid describes the behavior during the final stages of breakup. © 2000 Elsevier Science Ltd. All rights reserved.

1. Introduction

In part I, we investigated the effect of surfactants on the capillary instability of a liquid thread suspended in a quiescent ambient fluid, and of an annular layer coated on the interior of a circular tube, in the absence of a mean flow (Kwak and Pozrikidis, 2001). Consideration

* Corresponding author. Tel.: +1-858-534-6530; fax: +1-858-534-7078.
E-mail address: cpozrikidis@ucsd.edu (C. Pozrikidis).

0301-9322/01/$ - see front matter © 2000 Elsevier Science Ltd. All rights reserved.
PII: S0301-9322(00)00012-4

of the first problem was motivated, in part, by the significance of thread dynamics in the processes of fluid dispersion and mixing of immicible liquids by agitation. In practice, however, liquid threads typically arise from the filamentation of blobs or extended bubbles and drops in shear or elongational flow. The surface-tension induced amplification of disturbance causes the filaments to become unstable and eventually break up into arrays of primary and smaller satellite bubbles or drops. The presence of the ambient flow that is responsible for the filamentation is known to have a significant influence on the nature of the capillary instability, and thus on the size of the bubbles or drops resulting from the filament disintegration.

Several authors have studied the instability of a thread with constant surface tension extending under the influence of an ambient flow. Tomotika (1936) formulated the linear evolution problem for axisymmetric perturbations and for an axisymmetric extensional ambient flow, and discussed the long-time behavior. Mikami et al. (1975) improved Tomotika's theory, carried out numerical simulations of the linearized system of governing equations, and compared their numerical results with their laboratory observations. The presence of an extensional flow has three important consequences: it causes the unperturbed thread radius a to be reduced in time in a monotonic fashion; it causes the wavelength of a periodic perturbation to increase in time in a monotonic fashion; and it reduces the amplitude of the perturbation by interfacial stretching due to convection. The combination of the first two effects causes the reduced wave number of a perturbation, ka, to decrease monotonically during the evolution, and this renders the motion strongly dependent on the initial condition; $k = 2\pi/L$ is the wave number, and L is the wavelength of the perturbation.

The theoretical studies of Mikami et al. (1975) revealed that, under most conditions, a perturbation with a reduced wave number ka that is higher than unity initially decays; when ka becomes equal to unity, the perturbation starts growing with a time-dependent rate; finally, as ka tends to zero, the growth rate vanishes and then becomes negative, and the perturbation decays. If the amplitude of the perturbation happens to exceed the thread radius at some time during the period of transient growth, then breakup occurs at a finite time. The assumptions upon which the linear analysis relies, however, cease to be valid well before breakup, and the theoretical predictions of the conditions and time of breakup are only suggestive.

Khakhar and Ottino (1987) extended the analyses of Tomotika (1936) and Mikami et al. (1975) by considering an arbitrary linear ambient flow, which includes, as a special case, the axisymmetric elongational flow considered by the previous authors. Numerical solutions of the linearized evolution equations for simple shear flow and plane hyperbolic extensional flow showed that the structure of the ambient flow has a noticeable but not a profound effect on the nature of the instability.

In this paper, we extend the work of the previous authors in several ways. First, we discuss in more detail the special case of a viscous thread suspended in an inviscid ambient fluid and of an inviscid thread suspended in a viscous ambient fluid, and argue that, in these two cases, any perturbation is destined to grow at long times. Second, we extend the linear analysis to account for the presence of an immiscible surfactant that causes variations in surface tension according to a linear constitutive equation. In part I, it was shown that, in the absence of an ambient flow, a surfactant stabilizes an interface (Kwak and Pozrikidis, 2001). In this paper, we show that the increase in the mean level of the surface tension due to surfactant dilution leads to larger perturbation amplitudes at long times. Third, we carry out numerical simulations based on boundary-integral and finite-volume methods to describe the evolution of waves whose amplitude is not small compared to the thread radius, as required by linear theory, and thereby establish the behavior of the thread in the regime where the linearized approximation is not valid. Fourth, we develop a simplified system of equations that govern the evolution of a viscous thread suspended in an inviscid ambient fluid subject to long wavelength perturbations. The asymptotic model is an extension of that derived previously by Renardy (1994) and Papageorgiou (1995) for a thread suspended in a quiescent ambient fluid. Numerical solutions confirm that a similarity solution derived by Papageorgiou (1995) describes the behavior of the extended thread near the time and around the position of breakup even in the presence of extensional flow.

2. Problem statement and dimensional arguments

Consider an infinite thread of a Newtonian fluid with viscosity μ, designated as fluid 1, suspended in an unbounded ambient Newtonian fluid with viscosity $\lambda\mu$, designated as fluid 2, subject to an ambient axisymmetric elongational flow, as illustrated in Fig. 1. Gravitational forces are insignificant, and both the flow and the interface are required to remain axisymmetric at all times. The Reynolds number, defined with respect to the instantaneous thread radius and the maximum rate of elongation within the thread, is assumed so small that inertial effects are insignificant and the motion within the thread and ambient fluid is governed by the linear equations of Stokes flow.

The interface is populated by an insoluble surfactant that is convected by the interfacial velocity field and diffuses over the evolving interface but not into the bulk of the fluids. In

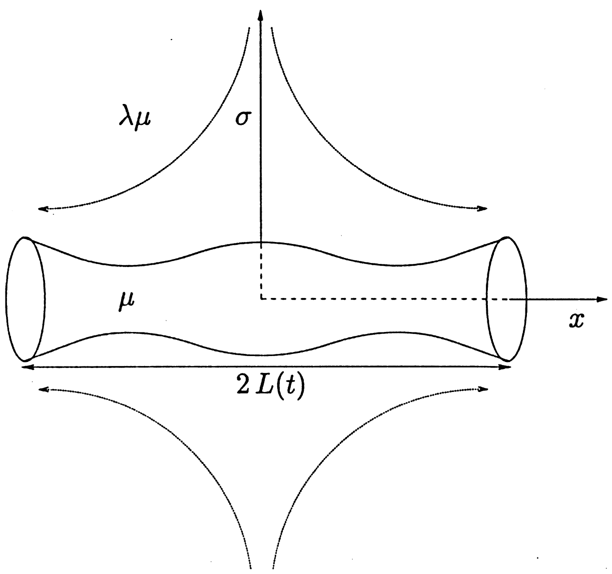

Fig. 1. Illustration of an infinite thread with viscosity μ surrounded by an ambient fluid with viscosity $\lambda\mu$, subject to an axisymmetric elongational flow.

polar cylindrical coordinates (x, σ, φ) with the x-axis coaxial with the thread, the evolution of the surfactant concentration Γ is governed by the convection-diffusion equation

$$\frac{\mathrm{d}\Gamma}{\mathrm{d}t} = -\boldsymbol{u}\cdot\boldsymbol{t}\,\frac{\partial\Gamma}{\partial l} - \frac{\Gamma}{\sigma}\frac{\partial(\sigma\boldsymbol{u}\cdot\boldsymbol{t})}{\partial l} - \Gamma 2\kappa_m\boldsymbol{u}\cdot\boldsymbol{n} + \frac{D_s}{\sigma}\frac{\partial}{\partial l}\left(\sigma\frac{\partial\Gamma}{\partial l}\right) \tag{1}$$

where the derivative $\mathrm{d}/\mathrm{d}t$ on the left-hand side expresses the rate of change following the motion of interfacial marker points moving with the component of the fluid velocity normal to the interface; l is the arc length along the trace of the interface in a meridional plane measured in the direction of the unit tangent vector $\boldsymbol{t}$, $\boldsymbol{n}$ is the unit normal vector pointing into the thread, κ_m is the mean curvature of the interface, and D_s is the surfactant diffusivity.

When the concentration of the surfactant lies below a saturation level, and variations in the surfactant concentration are sufficiently small, the surface tension γ is related to the surfactant concentration by Gibbs' equation

$$\gamma_c - \gamma = \Gamma RT \tag{2}$$

where R is the ideal gas constant, T is the absolute temperature, and γ_c is the surface tension of the clean interface in the absence of surfactants, (e.g., Adamson 1990). The sensitivity of the surface tension to the surfactant concentration is expressed by the dimensionless physicochemical parameter

$$\beta = \frac{\Gamma_r RT}{\gamma_c} \tag{3}$$

where the subscript r denotes a reference value. In terms of β, Eq. (2) takes the form

$$\gamma = \gamma_c\left(1 - \frac{\Gamma}{\Gamma_r}\beta\right) \tag{4}$$

Setting $\Gamma = \Gamma_r$, we obtain a relation between the reference surface tension and the surface tension of a clean interface,

$$\gamma_r = \gamma_c(1-\beta) \tag{5}$$

which may be substituted in Eq. (4) to give

$$\gamma = \frac{\gamma_r}{1-\beta}\left(1 - \frac{\Gamma}{\Gamma_r}\beta\right) \tag{6}$$

In the unperturbed state, the interface has a cylindrical shape with a circular cross-section of changing radius $a(t)$. The axial and radial components of the velocity inside and outside the thread are given by

$$u_x^\infty = G(t)\,x, \qquad u_\sigma^\infty = -\frac{1}{2}G(t)\,\sigma \tag{7}$$

where $G(t)$ is a specified time-dependent rate of elongation. Using the kinematic condition $\mathrm{d}a/\mathrm{d}t = u_\sigma$ ($\sigma = a$), we obtain a linear evolution equation for the thread radius,

$$\frac{da}{dt} = -\frac{1}{2}G(t)\,a \tag{8}$$

Assuming that the surfactant concentration is uniform, simplifying Eq. (1), and setting $\kappa_m = -1/(2a)$, we obtain an evolution equation for the surfactant concentration,

$$\frac{d\Gamma}{dt} = -\frac{1}{2}G(t)\,\Gamma \tag{9}$$

which shows that if the surfactant concentration is uniform at the initial instant, it will remain uniform at all times.

The pressure within the ambient fluid has the uniform but possibly time-dependent value $P^{\infty(2)}$, and the pressure within the thread has the uniform value $P^{\infty(1)} = P^{\infty(2)} + \gamma(t)/a(t)$. In polar cylindrical coordinates, the components of the stress tensor are given by

$$\sigma_{xx}^{\infty(1)} = -P^{\infty(1)} + 2\mu G, \quad \sigma_{x\sigma}^{\infty(1)} = 0,$$

$$\sigma_{\sigma x}^{\infty(1)} = 0, \quad \sigma_{\sigma\sigma}^{\infty(1)} = -P^{\infty(1)} - \mu G, \tag{10}$$

within the thread, and

$$\sigma_{xx}^{\infty(2)} = -P^{\infty(2)} + 2\lambda\mu G, \quad \sigma_{x\sigma}^{\infty(2)} = 0,$$

$$\sigma_{\sigma x}^{\infty(2)} = 0, \quad \sigma_{\sigma\sigma}^{\infty(2)} = -P^{\infty(2)} - \lambda\mu G, \tag{11}$$

within the ambient fluid. Note that the shear stress vanishes at the interface, whereas the normal stress undergoes a discontinuity determined by the surface tension, the local thread radius, the viscosity ratio, and the instantaneous rate of elongation.

Consider now the evolution of periodic axisymmetric perturbations in the radial position of the interface, and accompanying perturbations in the surfactant concentration. Linear stability analysis for a thread suspended in a quiescent ambient fluid reveals that when the reduced wave number ka is less than unity, where $k = 2\pi/L$ and L is the wavelength of the perturbation, the interface is unstable. The presence of surfactants reduces the growth rate of the perturbation but does not affect the range of unstable wave numbers, nor it is able to stabilize the flow (Kwak and Pozrikidis, 2001).

In the case of an extending thread, the axial velocity increases by the amount $G(t)\,L(t)$ over each period, and the wavelength $L(t)$ increases in time according to the equation

$$\frac{dL}{dt} = G(t)\,L \tag{12}$$

Correspondingly, the wave number is reduced in time according to the equation

$$\frac{dk}{dt} = -G(t)\,k \tag{13}$$

Thus, even if the initial wavelength corresponds to a reduced wave number ka that is stable, the diminishing radius of the thread, combined with the reduction in the wave number due to stretching, will ultimately bring ka into the unstable regime $ka < 1$, thereby rendering the thread susceptible to the capillary instability. The growth of interfacial waves in this regime, however, is opposed by the radially compressive action of the ambient flow. Our goal is to assess which mechanism will dominate at long times.

Consider first the instability of a clean interface. Working under the auspices of linear theory, we find, on the grounds of dimensional analysis, that the rate of change of the amplitude of a periodic wave, denoted as a_1, is given by

$$\frac{\mathrm{d}a_1}{\mathrm{d}t} = G(t)\left[-\frac{1}{2} + \frac{\lambda - 1}{\lambda + 1}\,\tilde{\Phi}(ka, \lambda)\right]a_1 + \frac{\gamma}{a\mu(\lambda + 1)}\,\tilde{\Sigma}(ka, \lambda)\, a_1 \tag{14}$$

where $\tilde{\Phi}$ is a dimensionless function of ka and λ, and $\tilde{\Sigma}$ is the normalized Rayleigh–Tomotika growth rate for a quiescent thread (Tomotika, 1935). When the viscosity ratio λ is equal to unity, the crests and troughs of an interfacial wave are convected passively by the elongational flow, and the term involving $\tilde{\Phi}$ on the right-hand side of Eq. (14) drops out. It is particularly significant to note that as λ tends to zero or to infinity, the location of the maximum of $\tilde{\Sigma}$ is shifted to zero, which means that the longer a wave, the faster it grows.

Using the evolution Eq. (8), we may transform Eq. (14) into an evolution equation for the ratio of the amplitude of the perturbation to the instantaneous mean thread radius,

$$\frac{\mathrm{d}}{\mathrm{d}t}\left(\frac{a_1}{a}\right) = G(t)\,\frac{\lambda - 1}{\lambda + 1}\,\tilde{\Phi}(ka, \lambda)\,\frac{a_1}{a} + \frac{\gamma}{a\mu(\lambda + 1)}\,\tilde{\Sigma}(ka, \lambda)\,\frac{a_1}{a} \tag{15}$$

If the ratio a_1/a becomes equal to unity at any time, the thread pinches off yielding two alternating arrays of drops.

Whether or not an interfacial wave will grow or decay is determined by the sign of the right-hand sides of Eqs. (14) or (15), which depends on the instantaneous thread configuration and thus on the history of the motion. At long times, ka tends to zero, the dimensionless functions $\tilde{\Phi}$ and $\tilde{\Sigma}$ behave as $k^2a^2 \ln(ka)$ for any finite and non-zero value of λ (Mikami et al., 1975, appendix I-A), the first term on the right-hand side of Eq. (14) dominates, and a_1 decays at an exponential rate. In contrast, for zero or infinite values of λ, corresponding to a viscous thread suspended in an inviscid ambient fluid or to an inviscid thread suspended in a viscous ambient fluid, as ka tends to zero, the dimensionless functions $\tilde{\Phi}$ and $\tilde{\Sigma}$ tend to constant values. At long times, the second term on the right-hand side of Eqs. (14) or (15) dominates, and a_1/a increases at an exponential rate leading to breakup at a finite time. These differences in the long time behavior underline the importance of the viscosity of either fluid.

Considering next the growth of perturbations in the presence of surfactants, we identify the reference values Γ_r and γ_r with the initial unperturbed values denoted, respectively, by $\Gamma_0(t = 0)$ and $\gamma_0(t = 0)$. Thus,

$$\beta = \frac{\Gamma_0(t = 0)RT}{\gamma_\mathrm{c}} \tag{16}$$

where the subscript 0 denotes the uniform values pertaining to the cylindrical thread.

Dimensionless analysis suggests that, in the context of linear theory, the rate of change of the amplitude of a periodic wave is governed by an equation of the form

$$\frac{\mathrm{d}a_1}{\mathrm{d}t} = G(t)a\left[-\frac{1}{2} + \frac{\lambda - 1}{\lambda + 1}\,\tilde{\Phi}(ka, \lambda)\right]\frac{a_1}{a} + \frac{\gamma_0(t)}{\mu(\lambda+1)}\,\tilde{\chi}\left(ka, \lambda, \beta, \alpha, \frac{\Gamma_0(t)}{\Gamma_0(t=0)}\right)\frac{a_1}{a}$$
$$+ \frac{\gamma_0(t=0)}{\mu(\lambda+1)}\,\tilde{\psi}\left(ka, \lambda, \beta, \alpha, \frac{\Gamma_0(t)}{\Gamma_0(t=0)}\right)\frac{\Gamma_1(t)}{\Gamma_0(t=0)} \tag{17}$$

where $\tilde{\chi}$ and $\tilde{\psi}$ are the dimensionless functions of their arguments, Γ_1 is the amplitude of the perturbation in the surfactant concentration, and we have introduced the dimensionless parameter

$$\alpha = \frac{a(t=0)\gamma_0(t=0)}{\mu D_s} \tag{18}$$

expressing the surfactant diffusivity. A similar equation can be written for Γ_1, and the system of the two linear evolution equations must be solved subject to an appropriate initial condition. When the rate of extension vanishes and the initial amplitudes of the interfacial deformation and surfactant concentration correspond to one of the two possible normal modes, the eigenvalues of the coefficient matrix of the linear system can be deduced from the dimensionless growth for a quiescent thread discussed by Kwak and Pozrikidis (2001).

The results of Kwak and Pozrikidis (2001) showed that the eigenvalues depend weakly on the parameters β, α, and $\Gamma_0/\Gamma_0(t=0)$ for a broad range of conditions, and may thus be approximated with the normalized Rayleigh–Tomotika growth rate $\tilde{\Sigma}$ introduced in Eq. (14). Now, the unperturbed surfactant concentration Γ_0 is reduced in time according to Eq. (9); accordingly, the unperturbed surface tension γ_0 increases in time according to Eq. (4). As a result, the presence of a surfactant raises the magnitude of the second term on the right-hand side of Eq. (17), and thereby promotes the amplification of the perturbation in the regime of unstable wave numbers. This prediction will be confirmed by the numerical solutions presented in the following sections.

3. Linear waves

To study the evolution of periodic perturbations whose amplitude is small compared to the instantaneous thread radius, we describe the radial position of the interface in the form

$$\sigma = f(x, t) = a(t) + \epsilon a_1(t)\cos(k(t)x) \tag{19}$$

where ϵ is a dimensionless number whose magnitude is small compared to unity, and $a_1(t)$ is the amplitude of the disturbance in the radial position. The surfactant concentration and surface tension are expressed in the analogous forms

$$\Gamma(x, t) = \Gamma_0(t) + \epsilon\Gamma_1(t)\cos(k(t)x) \tag{20}$$

and

$$\gamma(x, t) = \gamma_0(t) + \epsilon\gamma_1(t)\cos(k(t)x) \tag{21}$$

Substituting Eqs. (20) and (21) into constitutive Eq. (6), we find

$$\gamma_0(t) = \frac{\gamma_r}{1-\beta}\left(1 - \frac{\Gamma_0(t)}{\Gamma_r}\beta\right), \qquad \gamma_1(t) = -\frac{\gamma_r\beta}{1-\beta}\frac{\Gamma_1(t)}{\Gamma_r} \tag{22}$$

Next, we decompose the velocity within each fluid into an unperturbed component denoted as $\boldsymbol{u}^\infty$, given in Eq. (8), and a periodic disturbance component denoted as $\boldsymbol{u}^D$, so that

$$\boldsymbol{u}^{(j)} = \boldsymbol{u}^{\infty(j)} + \boldsymbol{u}^{D(j)} \tag{23}$$

for $j = 1, 2$, corresponding to the thread or ambient fluid. The axial and radial components of the disturbance velocity are related to the Stokes stream function Ψ_j by

$$u_x^{D(j)} = \epsilon\frac{1}{\sigma}\frac{\partial\Psi_j}{\partial\sigma}, \qquad u_\sigma^{D(j)} = -\epsilon\frac{1}{\sigma}\frac{\partial\Psi_j}{\partial x} \tag{24}$$

for $j = 1, 2$. Following the analysis of Kwak and Pozrikidis (2001), we find

$$\Psi_j(\sigma) = \sigma\big(A_{1,j}I_1(k\sigma) + B_{1,j}K_1(k\sigma) + A_{2,j}\sigma I_0(k\sigma) + B_{2,j}\sigma K_0(k\sigma)\big)\cos(k(t)x) \tag{25}$$

where $A_{1,j}$, $A_{2,j}$, $B_{1,j}$, and $B_{2,j}$ are constants, and I_0, K_0, I_1, K_1 are modified Bessel functions. Requiring a regular behavior at the thread axis and at infinity, we find that $B_{1,1}B_{2,1}$, $A_{1,2}$ and $A_{2,2}$ must vanish. Mikami et al. (1975) used an alternative form of the solution in terms of the modified Bessel functions I_1, K_1 and their first derivatives, but the two representations are equivalent with the present one being more convenient for algebraic manipulations.

We proceed by deriving and linearizing expressions for the cylindrical polar components of the velocity, pressure, normal vector, mean curvature, and surface tension with respect to ϵ. Substituting the simplified forms into the kinematic and dynamic boundary conditions, and then collecting and linearizing the resulting expressions, we obtain the linear algebraic system

$$\boldsymbol{M}\boldsymbol{w} = \boldsymbol{b} \tag{26}$$

for the vector

$$\boldsymbol{w}^{\mathrm{T}} = [A_1, A_2, B_1, B_2] \tag{27}$$

where, for simplicity, we have denoted $A_1 = A_{1,1}$, $A_2 = A_{2,1}$, $B_1 = B_{1,2}$, and $B_2 = B_{2,2}$. The coefficient matrix on the left-hand side of Eq. (26) is given by

$$\boldsymbol{M} = \begin{bmatrix} I_1(ka) & aI_0(ka) & -K_1(ka) & -aK_0(ka) \\ kI_0(ka) & kaI_1(ka)+2I_0(ka) & kK_0(ka) & kaK_1(ka)-2K_0(ka) \\ \mu kI_1(ka) & \mu\big(I_1(ka)+kaI_0(ka)\big) & -\lambda\mu kK_1(ka) & \lambda\mu\big(K_1(ka)-kaK_0(ka)\big) \\ \frac{\mu}{a}\big(kaI_0(ka)-I_1(ka)\big) & \mu kaI_1(ka) & \frac{\lambda\mu}{a}\big(kaK_0(ka)+K_1(ka)\big) & \lambda\mu kaK_1(ka) \end{bmatrix} \tag{28}$$

and right-hand side is given by

$$\boldsymbol{b}^{\mathrm{T}} = \left[0,\,0,\,\frac{3}{2}\mu(1-\lambda)Ga_1 - \frac{1}{2}\frac{\gamma_r\beta}{1-\beta}\frac{\Gamma_1(t)}{\Gamma_r},\,\frac{1}{2ka^2}\left(a_1\gamma_0(t)\,(1-k^2a^2)+a\,\gamma_r\frac{\beta}{1-\beta}\frac{\Gamma_1(t)}{\Gamma_r}\right)\right] \tag{29}$$

In the absence of surfactants, $\Gamma_1 = 0$, or when the surface tension is insensitive to the surfactant concentration, $\beta = 0$, we recover the results of Mikami et al. (1975, eqs. (3.6)) with some variations in the coefficient matrix due to the different expressions for the stream functions.

To describe the deformation of the interface, we require an evolution equation for the amplitude of the perturbation and for the amplitude of the surfactant concentration. To obtain the former, we require that the motion of point particles over the interface is consistent with the functional form (19), that is $D(\sigma - f)/Dt = 0$, where D/Dt is the material derivative, and find

$$\boldsymbol{u}_\sigma = \frac{\partial\sigma}{\partial t} + u_x\frac{\partial\sigma}{\partial z} \tag{30}$$

To obtain the latter, we use the surfactant convection–diffusion Eq. (1). Substituting the linearized expressions for the velocity, mean curvature, unit normal and tangent vectors into Eqs. (30) and (1), and linearizing all terms with respect to ϵ, we obtain three decoupled linear evolution equations for the wave number, unperturbed thread radius, and surfactant concentration

$$\frac{\mathrm{d}k}{\mathrm{d}t} = -G(t)k, \quad \frac{\mathrm{d}a}{\mathrm{d}t} = -\frac{1}{2}G(t)a, \quad \frac{\mathrm{d}\Gamma_0}{\mathrm{d}t} = -\frac{1}{2}G(t)\Gamma_0, \qquad (31))$$

and two coupled, highly nonlinear evolution equations for the disturbance amplitudes

$$\frac{\mathrm{d}a_1}{\mathrm{d}t} = -\frac{1}{2}G(t)a_1 + k\big[A_1I_1(ka) + A_2aI_0(ka)\big] \tag{32}$$

and

$$\frac{\mathrm{d}\Gamma_1}{\mathrm{d}t} = -\left(\frac{1}{2}G(t) + D_sk^2\right)\Gamma_1 + \Gamma_0(t)k\big\{A_1kI_1(ka) + A_2\big[2I_0(ka) + kaI_1(ka)\big]\big\} - \frac{1}{2}\frac{a_1}{a}\Gamma_0(t)(1-k^2a^2)G(t) - \Gamma_0(t)\frac{k}{a}\big(A_1I_1(ka) + A_2I_0(ka)\big) - \frac{1}{2}\frac{a_1}{a}\Gamma_0G(t) \tag{33}$$

Eqs. (31) show that the reduced wave number ka decreases monotonically and tends to vanish at long times. When the ambient fluid is quiescent corresponding to $G = 0$, the wave number, unperturbed thread radius, and unperturbed surfactant concentration are constant, the coefficients on the right-hand side of Eqs. (32) and (33) are independent of time, and the perturbation amplitudes $a_1(t)$ and $\Gamma_1(t)$ are exponential functions of time corresponding to normal modes. The growth rates were computed and graphed by Kwak and Pozrikidis (2001). More generally, the solution of system (32) and (33) must be found using numerical methods.

In the remainder of this paper, we confine our attention to a thread that is stretched at a constant rate. Treating G as a constant, we find that the wave number, unperturbed thread radius, and unperturbed surfactant concentration are exponentially decreasing functions of time given by

$$k(t) = k(t = 0)\,\mathrm{e}^{-Gt}, \quad a(t) = a(t = 0)\,\mathrm{e}^{-Gt/2}, \quad \Gamma_0(t) = \Gamma_0(t = 0)\,\mathrm{e}^{-Gt/2} \tag{34}$$

The reduced wave number is given by

$$ka(t) = (ka)(t = 0)\,\mathrm{e}^{-3Gt/2} \tag{35}$$

Substituting the expression for the unperturbed thread radius in Eq. (32), we obtain the more compact form

$$\frac{\mathrm{d}}{\mathrm{d}t}\left(\frac{a_1}{a}\right) = \frac{k}{a}\left[A_1 I_1(ka) + A_2 a I_0(ka)\right] \tag{36}$$

The coefficients A_1 and A_2 may be expressed as linear combinations of two parts: one part that is proportional to the rate of extension, and a second part that is proportional to the surface tension, as shown in Eq. (17). When the viscosities of the fluids are identical, the first part vanishes.

Eqs. (33) and (36) provide us with a linear non-autonomous system of ordinary differential equations for a_1 and Γ_1. Dimensional analysis shows that the solution depends on the viscosity ratio λ, the initial reduced wave number $(ka)(t = 0)$, the initial capillary number $Ca_0 = \mu Ga(t = 0)/\gamma_0$, the surfactant sensitivity parameter β defined in Eq. (16), the surfactant diffusivity property number defined in Eq. (18), and the initial ratio of the reduced amplitudes of the interface deformation and surfactant concentration, $\delta = (\Gamma_1/\Gamma_0)/(a_1/a)$ evaluated at $t = 0$. In the context of linear theory, the initial reduced amplitude of the interface deformation $(a_1/a)(t = 0)$ serves only as a scaling factor.

In the absence of surfactants, the solution of the linear system depends on λ, Ca_0, and $(ka)(t = 0)$. Mikami et al. (1975) and Khakhar and Ottino (1987) presented numerical results of an integrated version of Eq. (36) for several combinations of $(ka)\,(t = 0)$ and Ca_0, and for several non-zero and finite values of the viscosity ratio λ, confirming the predictions of the scaling arguments discussed in Section 2. The elongational flow causes the amplitude of a perturbation with a reduced wave number ka larger than unity to initially decrease in an exponential fashion; when ka reaches unity, the capillary instability reduces the rate of decay or even causes growth at a time-dependent rate; as ka tends to zero, the growth rate of the capillary instability tends to vanish and the elongational flow dominates causing exponential damping. Thus, as long as λ is finite and non-zero, the amplitude of the perturbation eventually decays yielding a thinning cylindrical thread at long times.

To illustrate the effect of surfactants, we consider the evolution of a thread for $\lambda = 1$, $Ca_0 = 0.1$, $\delta = 1$, and for several reduced initial wave numbers $(ka)(t = 0) = 1, 2, 3, 4, 5$, considered by examined by Mikami et al. (1975). All numerical results were obtained using the second-order Runge-Kutta method implemented with a constant time step. Numerical simulations for clean and polluted interfaces with $\beta = 0.5$ and $\alpha = 100$ showed that the disturbance initially decays faster in the presence of a surfactant than it does for a clean interface, for the following two reasons. First, a surfactant stabilizes a thread suspended in an quiescent fluid, that is, it reduces its growth rate (Kwak, and Pozrikidis 2001). Second, the extensional flow causes surfactant dilution and thus raises the mean level of the surface tension; the higher the surface tension, the faster the rate of decay. When, however, the interface becomes unstable for $(ka)(t) < 1$, these two effects work in opposite ways; the first one reduces the growth rate of the instability, and the second one promotes it. As a result, at long times, the amplitude of the perturbation in the presence of a surfactant is higher than that for a clean interface, except when $(ka)(t = 0) = 5$. This exception is due to the subtle competition of the two aforementioned effects during the early stages of the evolution.

Next, we examine the effect of the capillary number Ca_0 for a neutrally stable initial reduced wave number $(ka)(t = 0) = 1$. Simulations have shown that below a critical capillary number that depends on the physical parameters, the capillary instability dominates and the thread breaks up into a perfectly periodic series of drops (Kwak 1999). When Ca_0 is raised above the critical value, the disturbance grows temporarily, reaches a maximum, and then it decays under the influence of the elongational flow. For higher values of Ca_0 the damping action of the elongational flow dominates at the outset, and the amplitude of the disturbance decays at short and long times. For $\lambda = 1$, $\beta = 0.5$, $\alpha = 100$, and $\delta = 1$, the critical capillary number is estimated to be $Ca_0 = 0.05$. Eq. (14) suggests that the rate of decay is proportional to the instanteneous thread radius.

Next, we address the effect of the surfactant sensitivity parameter β, defined in Eq. (16). The numerical results have shown that raising β reduces the growth rate of the disturbance during the early stages of the motion, but the stabilizing effect diminishes or even disappears at long times. Once again, the increase in the mean surface tension due to surfactant dilution promotes the capillary instability; raising β causes the amplitude of the perturbation to reach higher levels at long times. When $\lambda = 0$, the perturbation keeps growing, eventually causing the thread to pinch off at the troughs of the periodic wave at long times. In constrast, when $\lambda = 1$, the perturbation eventually decays. These differences corroborate the arguments of Section 2 regarding the singular behavior occurring when either the thread or the ambient fluid is inviscid.

Fig. 2 illustrates the effect of the surfactant diffusion parameter α defined in Eq. (18) for $\lambda = 1$, $Ca_0 = 0.1$, $\beta = 0.5$, $(ka)(t = 0) = 1$, and $\delta = 1$; the solid lines correspond to a clean interface. The lower the value of α, the higher the surfactant diffusivity and the more uniformly the surfactant is distributed over the interface. Comparing the growth curves for the various values of α displayed in this figure, we find that reducing the surfactant diffusivity, and thus allowing the establishment of stronger surfactant concentration gradients, initially reduces the

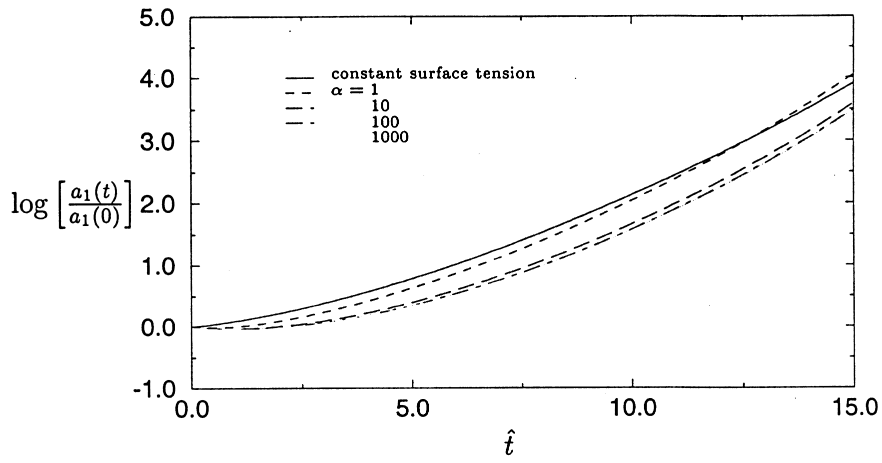

Fig. 2. Evolution of the amplitude of a contaminated interface with $\lambda = 1$, $\beta = 0.5$, $\delta = 1$, $Ca_0 = 0.1$, $(ka)(t = 0) = 0.9$, and $(a_1/a)(t = 0) = 0.01$, for $\alpha = 1$, 10, 100, 1000.

growth rate of the perturbation, in agreement with the results of Kwak and Pozrikidis (2001) for an unstretched interface. Dilution of the surfactant, however, smears out the concentration gradients and diminishes the significance of the surfactant diffusivity at long times. For $\lambda = 0$, the amplitude of the disturbance grows monotonically at long times in agreement with the arguments in Section 2.

4. Boundary-integral simulations

Linear theory predicts that the thread is overall stable when the viscosity ratio λ is non-zero and non-infinite, and unstable otherwise. For non-zero and finite values of λ, the presence of a surfactant initially reduces the growth rate of a disturbance, but the reduction of the surfactant concentration at long times, due to interfacial stretching, raises the mean level of the surface tension and allows the perturbation to survive for a longer period of time. Linear theory may cease to be valid during a certain stage of the evolution when the amplitude of the perturbation is no longer infinitesimal. To account for this occurrence, we investigate the non-linear evolution using a boundary-integral method.

To formulate the numerical method, we decompose the flow in an unperturbed and a disturbance component, as shown in Eq. (23). The disturbance velocity satisfies the integral equation

$$u_\alpha^D(\boldsymbol{x}_0) = \frac{2}{1+\lambda}\left(-\frac{1}{8\pi\mu_1}\int_C G_{\alpha\beta}(\boldsymbol{x},\boldsymbol{x}_0)\,\Delta f_\beta^D(\boldsymbol{x})\,\mathrm{d}l(\boldsymbol{x}) + \frac{1-\lambda}{8\pi}\int_C^{PV} Q_{\alpha\beta\gamma}(\boldsymbol{x},\boldsymbol{x}_0)\,u_\beta^D(\boldsymbol{x})\,n_\gamma(\boldsymbol{x})\,\mathrm{d}l(\boldsymbol{x})\right) \quad (37)$$

where point $\boldsymbol{x}_0$ lies in the interface, Greek subscripts, α, β, and γ, run over the axial and radial polar cylindrical coordinates x or σ, C is one period of the contour of the interface in a meridional plane, l is the arc length along C, $\boldsymbol{n}$ is the unit normal vector to the interface pointing into the thread, PV denotes the principal value of the double-layer integral, and the kernels $\boldsymbol{G}$ and $\boldsymbol{Q}$ are the velocity and stress periodic Green's functions of axisymmetric Stokes flow (Pozrikidis, 1992).

The density of the single-layer potential $\Delta \boldsymbol{f}^D$ is the disturbance component of the jump in the interfacial traction, defined as

$$\Delta \boldsymbol{f}^D = \boldsymbol{f}^{D(1)} - \boldsymbol{f}^{D(2)} = \left(\boldsymbol{\sigma}^{D(1)} - \boldsymbol{\sigma}^{D(2)}\right) \cdot \boldsymbol{n} \tag{38}$$

where $\boldsymbol{\sigma}^{D(1)}$ and $\boldsymbol{\sigma}^{D(2)}$ are, respectively, the disturbance stress tensor in the thread and ambient fluid. Combining the decomposition $\Delta \boldsymbol{f}^D = \Delta \boldsymbol{f} - \Delta \boldsymbol{f}^\infty$ with the interfacial traction jump condition $\Delta \boldsymbol{f} = \gamma 2\kappa_m \boldsymbol{n} - (\boldsymbol{I} - \boldsymbol{nn}) \cdot \nabla\gamma$, and using expressions (10) and (11), we find

$$\Delta \boldsymbol{f}^D = \gamma 2\kappa_m \boldsymbol{n} - (\boldsymbol{I} - \boldsymbol{nn}) \cdot \nabla\gamma - \mu G(1-\lambda)\,(2n_x \boldsymbol{e}_x - n_\sigma \boldsymbol{e}_\sigma) \tag{39}$$

The numerical method for solving the integral Eq. (37) and simultaneously integrating the convection-diffusion equation for the concentration of the surfactant, Eq. (1), is discussed by Kwak and Pozrikidis (2001). The demands on CPU time, however, are substantially higher due to the exponential increase of the domain of computation. A typical simulation requires approximately 72 h of CPU time on a SUN SPARCstation 20 workstation. All numerical results presented in this section correspond to a constant rate of elongation G.

First, we consider a thread with a clean interface for $\lambda = 1$, $(a_1/a)(t=0) = 0.2$, $Ca_0 = 0.1$, and initial wave numbers $(ka)(t=0) = 1$, 2, 3, 4, and 5, and confirm consistency with the predictions of linear theory. Fig. 3 shows the evolution of the reduced amplitude of the interface, $a_1(t)/a_1(t=0)$, plotted against the instantaneous reduced wave number $(ka)(t)$ on a log-linear scale. The solid lines correspond to the boundary-integral simulations, and the dashed lines correspond to the predictions of linear theory. The figure shows that the disturbance is eventually stabilized by the extensional flow, with a brief period of growth occurring when the reduced wave number is less than, but close to, unity. The agreement

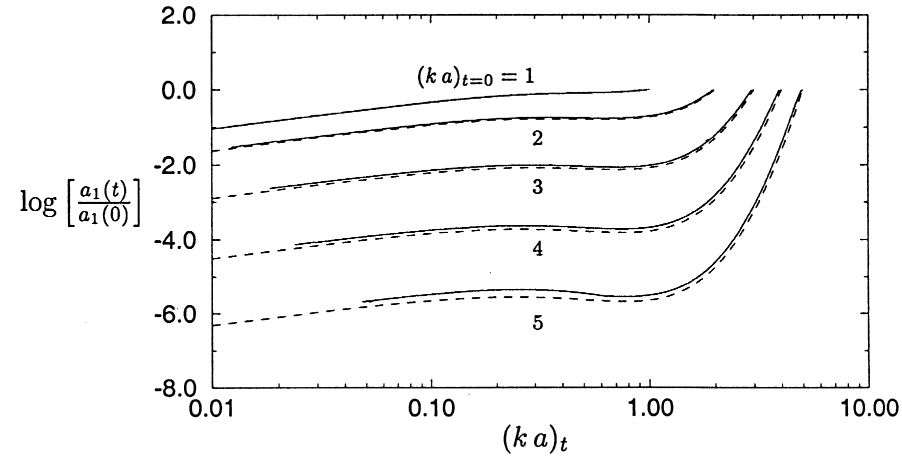

Fig. 3. Evolution of the disturbance amplitude computed by the boundary integral method (solid lines) or by the linear theory of Mikami et al. (dashed lines) for a thread with $\lambda = 1$, $\beta = 0$ (clean interface), for $Ca_0 = 0.1$, $(a_1/a)(t = 0) = 0.2$ and $(ka)(t = 0) = 1$, 2, 3, 4, and 5.

between the numerical results and the linearized predictions is good even though the amplitude of the perturbation may not be negligible compared to the thread radius.

Next, we consider the effect of the strength of the ambient flow. For low values of Ca_0, corresponding to a weak flow, the thread breaks up into two alternating series of primary and secondary drops. The ratio of the volume of the primary drops to the volume of the secondary drops decreases as Ca_0 is raised. This trend is consistent with the results of boundary-integral simulations by Kwak and Pozrikidis (2001) in the absence of an elongational flow, which showed that the volume ratio increases monotonically with the wavelength of the perturbation.

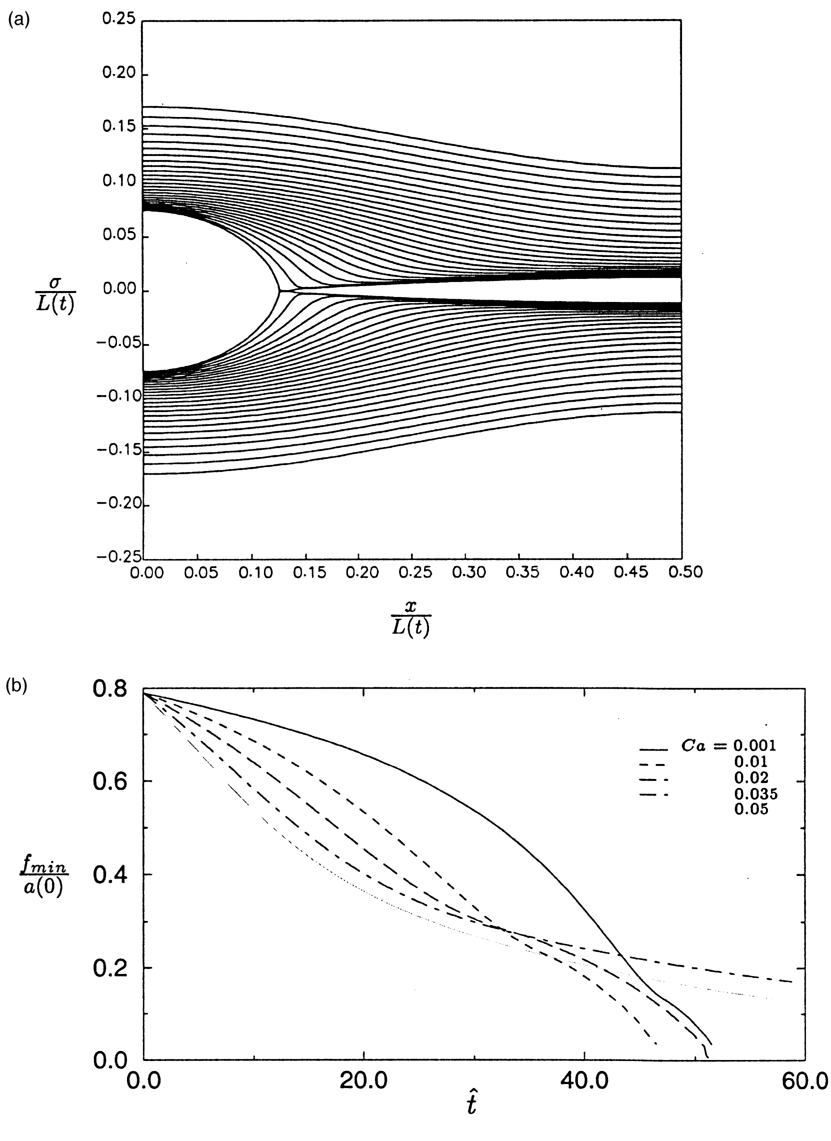

Fig. 4. (a) Characteristic stages in the evolution of a thread for $\lambda = 1$, $\beta = 0$ (clean interface), $(ka)(t = 0) = 0.9$, $(a_1/a)(t = 0) = 0.2$ and $Ca_0 = 0.02$. (b) Corresponding minimum thread radius.

The analogy is made by noting that the higher the capillary number, the longer the wavelength of the perturbation at the time of breakup. When the capillary number exceeds the critical capillary number, as discussed in Section 3, the extensional flow suppresses the growth of the perturbations and breakup does not occur during the length of the simulation, although a small waviness persists at long times. This behavior is consistent with the predictions of linear theory discussed in Section 2. As an example, in Fig. 4(a), we present a sequence of interfacial profiles for $\lambda = 1$, $(ka)(t = 0) = 0.9$, $Ca_0 = 0.02$, and for a moderate initial disturbance amplitude $(a_1/a)(t = 0) = 0.2$.

Fig. 4(b) shows the evolution of the minimum thread radius corresponding to the capillary numbers $Ca_0 = 0.001$, 0.01, 0.02, 0.035, and 0.05. For $Ca_0 \leq 0.001$, the capillary instability dominates at all times, the growth curve is concave downward, and the thread breaks up at a finite time yielding a series of drops. It is interesting to note that the breakup time is a non-monotonic function of Ca_0. For example, when $Ca_0 = 0.01$, the thread breaks up faster than it does for $Ca_0 = 0$, in agreement with the observations of Grace (1982). As Ca_0 is raised, the critical time decreases, reaches a minimum, and then tends to infinity at a critical capillary number. For $Ca \geq 0.035$, the extensional flow dominates at all times, and the amplitude of the interface decays in a nearly exponential fashion, in agreement with the predictions of linear analysis discussed in Section 3. In the intermediate range of capillary numbers, the growth curve is initially concave downward due to the capillary instability, but then it develops an inflection point and decays exponentially at long times.

Next, we consider the evolution of the extending thread in the presence of a surfactant. Fig. 5 illustrates the evolution of the reduced minimum radius plotted with respect to time for $\lambda = 0$, corresponding to a viscous thread suspended in an inviscid ambient fluid, $\beta = 0.5$, $\alpha = 100$, $(ka)(t = 0) = 0.9$, $Ca_0 = 0.01$ corresponding to a weak elongational flow, and for a small perturbation amplitude $(a_1/a)(t = 0) = 0.01$. The solid lines represent the boundary-integral simulations, and the dashed lines represent the predictions of linear theory. To illustrate the

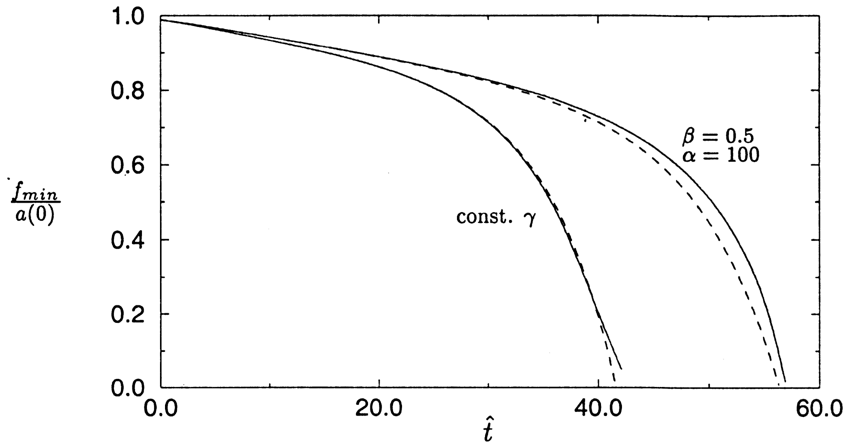

Fig. 5. Minimum thread radius for $\lambda = 0$, $\beta = 0.5$, $\alpha = 100$, $(ka)(t = 0) = 0.9$, $(a_1/a)(t = 0) = 0.01$ and $Ca_0 = 0.01$. The solid lines represent numerical simulations based on the boundary integral method, and the dashed lines represent the predictions of the linear theory.

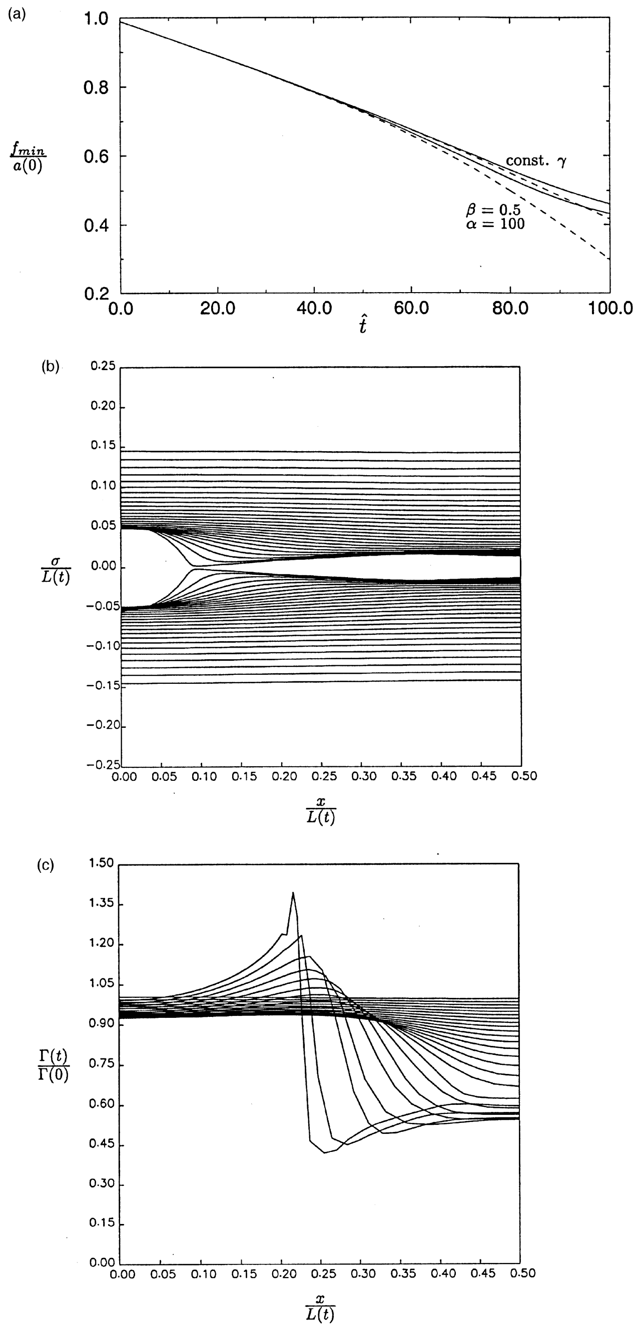

Fig. 6. (a) Minimum thread radius for $\lambda = 1$, $\beta = 0.5$, $\alpha = 100$, $(ka)(t = 0) = 0.9$, $(a_1/a)(t = 0) = 0.01$ and $Ca_0 = 0.01$. The solid lines represent numerical simulations based on the boundary integral method, and the dashed lines represent the predictions of the linear theory. (b) and (c) Characteristic stages in the evolution of the thread and surfactant concentration.

effect of the surfactant, we have included results for a clean interface corresponding to $\beta = 0$. The results show that the surfactant stabilizes the thread during the early stages of the motion, but the amplitude of the disturbance starts growing at $\hat{t} \sim 10$, and the thread breaks up into drops at long times. Fig. 5 shows the evolution of the minimum thread radius, revealing that the critical time for breakup increases by approximately 35% in the presence of the surfactant. In addition to affecting the critical time of breakup, the surfactant initiates non-linear interactions at an earlier stage of the motion, and the numerical simulation diverges from the linear prediction earlier than it does for a clean interface.

Fig. 6(a) is the counterpart of Fig. 5 for $\lambda = 1$. Comparison of the two cases reveals that when the viscosity of the ambient fluid is comparable to that of the thread, the surfactant promotes the growth of the interfacial waves, although the effect is small. In addition, significant discrepancies between the linear predictions and the numerical simulations occur at long times, with the effect of the surfactant being overestimated by linear theory. To illustrate the reason for these discrepancies, in Fig. 6(b) we present typical stages in the evolution of the interface, and in Fig. 6(c) we show the corresponding evolution of the surfactant concentration. Note that the profiles have been rescaled with respect to the instantaneous wavelength. Several features are worth noting: as in the case of a clean interface, the thread breaks up asymmetrically yielding two alternating series of drops; because of the long evolution time until breakup, the ratio of the volume of the primary and secondary drops is small; and the extensional flow causes the formation of an unduloid on the secondary drop.

As a final topic, we examine the effect of the initial amplitude of the perturbation on thread breakup. Numerical simulations have shown that a weak elongational flow does not alter the general features of the evolution when $\lambda = 0$. However, when $\lambda = 1$, the thread breaks up into three alternating arrays of drops in the absence of elongational flow, but forms a drop-spindle structure in the presence of elongational flow, as it does under constant surface tension. In physical terms, dilution of the surfactant due to interface stretching prevents the formation of tertiary drops.

Fig. 7 illustrates the evolution of the minimum thread radius, confirming the behavior

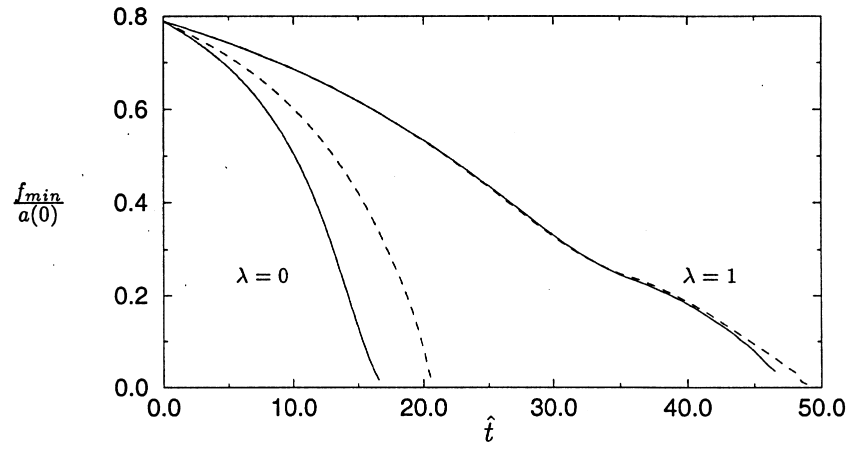

Fig. 7. Evolution of the minimum thread radius for a clean interface (solid lines) and a polluted interface with $\beta = 0.5$, $\alpha = 100$ (dotted lines) for $\lambda = 0, 1$, and $(ka)(t = 0) = 0.9$, $(a_1/a)(t = 0) = 0.2$, and $Ca_0 = 0.01$.

discussed earlier on the basis of Figs. 4 and 5; the polluted interface is represented by a dashed line, and the clean interface is represented by a solid line. The presence of a surfactant delays the break up time for $\lambda = 0$, but its effect is insignificant for $\lambda = 1$.

5. Local dynamics near break up

In this section, we turn our attention to the evolution of a viscous thread suspended in an inviscid ambient fluid, subject to long wave-length perturbations, and discuss the predictions of a simplified system of governing equations based on long-wave asymptotics. This analysis extends previous work by Renardy (1994), Papageorgiou (1995) and Brenner et al. (1996), which is applicable for a thread suspended in a quiescent ambient fluid. In fact, only simple modifications are necessary to account for an ambient axisymmetric extensional flow. Analogous model systems for Navier–Stokes flow have been developed by Eggers (1997); the extension of the inertial model to include stretching due to ambient flow is straightforward.

Papageorgiou (1995) and Brenner et al. (1996) showed that in the absence of stretching, corresponding to $Ca_0 = 0$, the asymptotic equations admit a family of similarity solutions which predict that breakup occurs at a finite time. Pozrikidis (1999) confirmed the physical relevance of the least unstable similarity solution by comparing its predictions with numerical simulations based on the boundary-integral method. This similarity solution reveals that the velocity field and viscous stresses tend to become singular near the point of breakup at the critical time. Because of this singularity, the viscous stresses associated with the motion induced by capillarity become increasingly stronger than those of the non-singular imposed extensional flow, and the similarity solution developed by Papageorgiou (1995) is expected to become asymptotically valid even in the presence of an extensional flow.

To confirm the relevance of the similarity solution near the critical time of breakup, we performed numerical simulations based on it, and compared the results with numerical simulations conducted using the boundary-integral method. In the absence of a surfactant, the fundamental assumptions of the long wave model are: (a) the shear stress vanishes at the interface, (b) the slope of the interface $\partial f/\partial x$ is small compared to unity, where the equation $\sigma = f(x, t)$ describes the position of the interface, and (c) the pressure within the thread p and axial velocity u_x are independent of the radial position σ. To derive the model system, we may either pursue the integral balance approach of Renardy (1994), or the formal long-wave asymptotics approach of Papageorgiou (1995). Either way, we derive the simplified equations

$$\frac{\partial f}{\partial t} + u_x \frac{\partial f}{\partial x} + \frac{1}{2}\frac{\partial u_x}{\partial x} f = 0 \tag{40}$$

and

$$\frac{3\mu}{2} f \frac{\partial^2 u_x}{\partial x^2} + 3\mu \frac{\partial u_x}{\partial x}\frac{\partial f}{\partial x} + \frac{\gamma}{2f}\frac{\partial f}{\partial x} = 0 \tag{41}$$

which are identical to those derived by the previous authors in the absence of an elongational flow. Note that Eq. (40) is consistent with Eq. (30) for an unperturbed interface. The presence of a surfactant may be included by adding an appropriate term to the left-hand side of Eq. (41) expressing the Marangoni shear stress at the interface, while also supplementing Eqs. (40) and (41) by a convection-diffusion equation for the surfactant concentration. Kwak and Pozrikidis (2001) presented strong evidence that the presence of surfactants does not affect the nature of the evolution in the absence of external stretching; a similar insensitivity is expected in the presence of an ambient flow.

To simplify the discussion, we confine our attention to a thread that is stretched at a constant rate corresponding to a constant rate of elongation G. To isolate the effect of the extensional flow, we introduce the dimensionless Lagrangian axial coordinate

$$\xi = \frac{x}{a_0} \exp\left(- Ca_0 \hat{t} \right) \tag{42}$$

where $\hat{t} = \gamma t / \mu a_0$ is the dimensionless time, $a_0 = a(t = 0)$ is the initial thread radius, $Ca_0 = \mu G a_0 / \gamma$ is the initial capillary number, and γ is the constant and uniform surface tension.

Furthermore, we express the position of the interface and axial velocity in the forms

$$f = a_0 \tilde{f}(\xi, \hat{t}) \exp\left(- \frac{1}{2} Ca_0 \hat{t} \right) \tag{43}$$

and

$$u_x = Gx + \frac{\gamma}{\mu} \tilde{u}_x(\xi, \hat{t}) \exp\left(Ca_0 \hat{t} \right) \tag{44}$$

where $\tilde{f}$ and $\tilde{u}_x$ are periodic functions of ξ with reduced wavenumber ka. The undisturbed stretched cylindrical interface corresponds to the flat distributions $\tilde{f} = 1$ and $\tilde{u}_x = 0$.

Substituting expressions (42)–(44) into Eqs. (40) and (41), we derive the dimensionless equations

$$\frac{\partial \tilde{f}}{\partial \hat{t}} + \tilde{u}_x \frac{\partial \tilde{f}}{\partial \xi} + \frac{1}{2} \frac{\partial \tilde{u}_x}{\partial \xi} \tilde{f} = 0 \tag{45}$$

and

$$\frac{3}{2} \tilde{f} \frac{\partial^2 \tilde{u}_x}{\partial \xi^2} + 3 \frac{\partial \tilde{u}_x}{\partial \xi} \frac{\partial \tilde{f}}{\partial \xi} + 3 Ca_0 \frac{\partial \tilde{f}}{\partial \xi} + \frac{1}{2 \tilde{f}} \frac{\partial \tilde{f}}{\partial \xi} \exp\left(\frac{1}{2} Ca_0 \hat{t} \right) = 0 \tag{46}$$

The effect of the extensional flow is manifested in the third and fourth terms on the left-hand side of Eq. (46). The model system comprising of Eqs. (45) and (46) was solved by a spectral collocation method similar to that used by Papageorgiou (1995), keeping 20 Fourier components in space, and using a second order Runge-Kutta scheme for the time integration.

As a case study, we consider the evolution of the minimum thread radius for $Ca_0 = 0.01$ corresponding to a weak extensional flow, and a small amplitude perturbation $(a_1/a)(t = 0) = 0.01$ with initial reduced wave number $(ka)(t = 0) = 0.9$. Results obtained on the basis of long-wave approximation and the boundary integral method show significant discrepancies during the early stages of the motion. As, however, the wave amplifies, respective graphs of the minimum radius show a common slope equal to −0.0709 which is in agreement with the theoretical prediction of Papageorgiou (1995). Fig 8(a) shows corresponding results for a stronger extensional flow at $Ca_0 = 0.1$, and identical conditions otherwise. The dashed line shows results obtained by the long-wave approximation, the solid line shows results obtained by the boundary integral method, and the long dashed line shows results obtained by the linear approximation. Due to rapid stretching of the thread, the agreement among the three predictions is good over an extended period of time. The predictions of the long-wave model are consistent with those of the boundary-integral simulation, both corroborating the dominance of the similarity solution near the critical time. All three simulations predict breakup at a finite critical time.

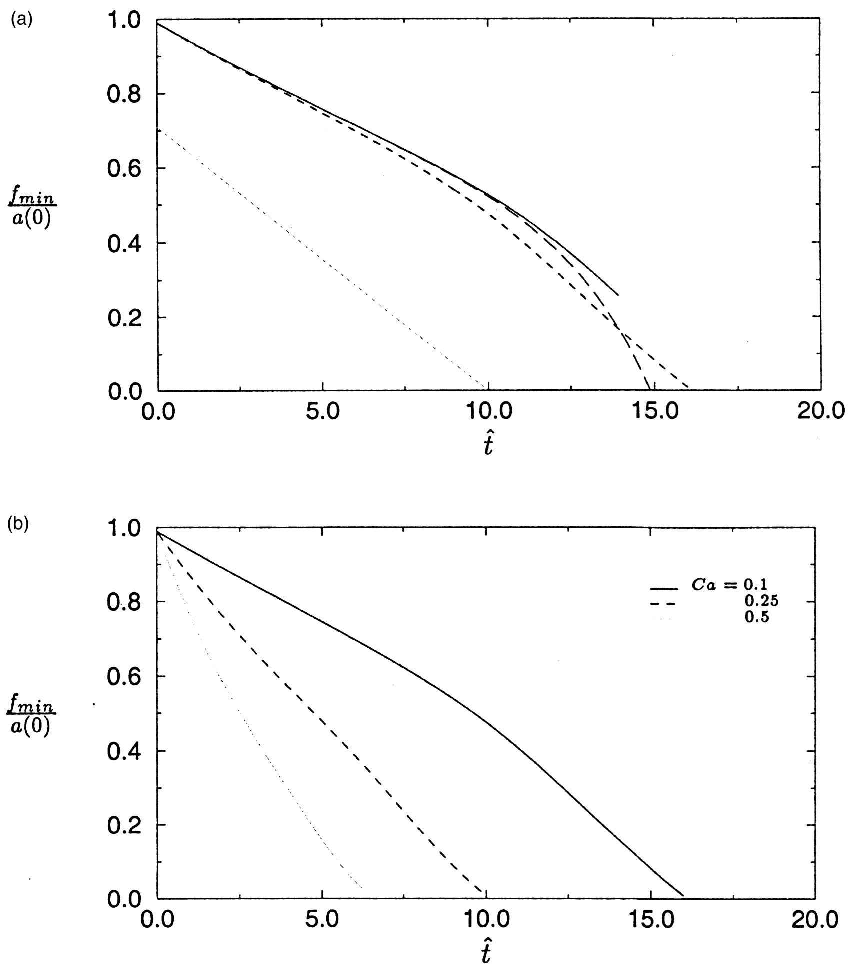

Fig. 8. Minimum thread radius predicted by numerical simulations based on the boundary integral method (solid line), the long-wave model (dashed line), linear theory (long dashed line), for $\lambda = 0$, $(ka)(t = 0) = 0.9$, and $(a_1/a)(t = 0) = 0.01$; (a) $Ca_0 = 0.1$: the straight dashed line corresponds to Papageorgiou's similarity solution. (b) Evolution of the minimum thread radius computed by the long-wave model for $\lambda = 0$, $(ka)(t = 0) = 0.9$, $(a_1/a)(t = 0) = 0.01$; and $Ca_0 = 0.1, 0.25$, and 0.5.

Fig. 8(b) shows a family of numerical solutions based on the long wave model for higher values of Ca_0. For large values of Ca_0, the extensional flow dominates at short and moderate times, causing the minimum thread radius to decay at an exponential rate. As the thread radius is reduced, the capillary pressure γ/a is raised and finally exceeds the constant magnitude of the viscous stresses of the imposed elongational flow; this occurs when $a \approx \delta a_0/Ca_0$, where δ is a dimensionless coefficient. Beyond that time, the similarity solution dominates the local dynamics causing the development of an inflection point. The data in Fig. 8(b) suggest that the constant δ is on the order of 100.

6. Discussion

We have found that, in the context of linear theory, a perturbation with a sufficiently small initial amplitude decays at long times, as long as neither the viscosity of the thread nor the viscosity of the ambient fluid is equal to zero. If the viscosity of either fluid is non-zero, perturbations of sufficiently small amplitude are stabilized by stretching due to convection. The limit of zero or infinite viscosity ratio has been shown by previous authors to be singular with regard to thread breakup in a quiescent fluid; for any value of the viscosity ratio but zero and infinity, breakup occurs in an asymmetric manner with the interface forming conical structures on either side of the point of minimum radius; for zero viscosity ratio, breakup occurs in a symmetric fashion (Pozrikidis 1999, Lister and Stone 1998).

In practice, the viscosity ratio is finite, however small, and stretching due to an ambient flow or thread elongation should be able to suppress the growth of small perturbations, but not necessarily the growth of finite-amplitude perturbations. A liquid thread subtended between two rods forms a bridge that may be stretched by translating one or both of the rods in the axial direction. If the relative velocity of translation is constant, then the rate of elongation is reduced as the inverse of time. The linear analysis of Section 3 suggests that even in this case of weak stretching, the thread will not break up at a finite time when both fluids are viscous. In practice, however, nonlinear effects due to finite interface deformation and fluid inertia become important when the thread has suffered substantial deformation during the period of transient growth, and may allow for amplification leading to thread disintegration. Thus, in practice, unless large disturbances are screened out, or the rate of elongation is sufficiently large, breakup may occur for any value of the viscosity ratio including zero and infinity.

We have found that, because of an increase in the average value of the surface tension due to surfactant dilution, a surfactant has an overall destabilizing influence on an extended thread especially for small values of the viscosity ratio. Perturbations may grow during a permanent or transient unstable period, with the wave numbers dominating during that period depending on the initial condition. In contrast, in the absence of stretching, the most dangerous mode is selected on the basis of maximum growth rate irrespective of the initial condition. Mikami et al. (1975) established a criterion for wave number selection on a thinning thread based on the behavior of the relative amplification, defined as the ratio of the instantaneous disturbance amplitude to the minimum amplitude occurring during the evolution. If a minimum does not occur, or if the instantaneous wave number is larger than the one corresponding to the minimum, then the relative amplification is set equal to zero. The most unstable wave number at any instant corresponds to the maximum amplification rate; breakup occurs when the maximum disturbance amplitude becomes equal to the thread radius. The ratio of the minimum disturbance amplitude to the initial thread radius is an unspecified parameter. Khakhar and Ottino (1987) proposed that the minimum disturbance amplitude should be set equal to the molecular displacement associated with thermal fluctuations.

Mikami et al. (1975) and Khakhar and Ottino (1987) found that the aforementioned criterion gives good agreement between theoretical predictions and laboratory observations, although the comparisons are hindered by the fact that breakup does not occur simultaneously over the entire length of the thread, and the spacing between the drops is not constant. We have not been able to identify experiments describing the effect of a surfactant. The present work, however, suggests that since surfactants have a significant influence on the minimum disturbance amplitude and most dangerous instantaneous wave number, they will also have a significant influence on the time of breakup and on the resulting drop density distribution. Specifically, a surfactant should cause breakup to occur at an earlier time.

Acknowledgements

This research is supported by a grant provided by the National Science Foundation.

References

Adamson, A.W., 1990. Physical Chemistry of Surfaces. Wiley, New York.

Brenner, P.M., Lister, J.R., Stone, H.A., 1996. Pinching threads, singularities and the number 0.0304. Phys. Fluids 8, 2827–2836.

Eggers, J., 1997. Nonlinear dynamics and breakup of free-surface flows. Rev. Modern Phys. 69, 865–930.

Grace, H.P., 1982. Dispersion Phenomena in high viscosity immiscible fluid systems and application of static mixers as dispersion devices in such systems. Chem. Eng. Commun. 14, 225–277.

Khakhar, D.V., Ottino, J.M., 1987. Breakup of liquid threads in linear flows. Int. J. Multiphase Flow 13, 71–86.

Kwak, S., Pozrikidis, C., 2001. Effect of surfactants on the instability of a liquid thread or annular layer. Part I: Quiescent fluids. Int. J. Multiphase Flow 27, 1–38.

Lister, J.R., Stone, H.A., 1998. Capillary breakup of a viscous thread surrounded by another viscous fluid. Phys. Fluids 10, 2758–2764.

Mikami, T., Cox, R.G., Mason, S.G., 1975. Breakup of extending liquid threads. Int. J. Multiphase Flow 2, 113–138.

Papageorgiou, D.T., 1995. On the breakup of viscous liquid threads. Phys. Fluids 7, 1529–1544.

Pozrikidis, C., 1992. Boundary integral and singularity methods for linearized viscous flow. Cambridge University Press, Cambridge.

Pozrikidis, C., 1999. Capillary instability and breakup of a viscous thread. J. Eng. Math. 36, 255–275.

Renardy, M., 1994. Some comments on the surface-tension driven break-up (or the lack of it) of viscoelastic jets. J. Non-Newtonian Fluid Mech. 51, 97–107.

Tomotika, S., 1935. On the instability of a cylindrical thread of a viscous liquid surrounded by another viscous fluid. Proc. Roy. Soc. A 150, 322–337.

Tomotika, S., 1936. Breaking up of a drop of viscous liquid immersed in another viscous fluid which is extending at a uniform rate. Proc. Roy. Soc. A 153, 302–318.